



The uric acid crystal receptor Clec12A potentiates type I interferon responses

Kai Li^{a,b}, Konstantin Neumann^c, Vikas Duhan^d, Sukumar Namineni^e, Anne Louise Hansen^f, Tim Wartewig^a, Zsuzsanna Kurgyis^a, Christian K. Holm^f, Mathias Heikenwalder^{e,g}, Karl S. Lang^d, and Jürgen Ruland^{a,b,h,1}

^aInstitut für Klinische Chemie und Pathobiochemie, Klinikum rechts der Isar, Technische Universität München, 81675 Munich, Germany; ^bGerman Center for Infection Research (DZIF), Partner Site Munich, 81675 Munich, Germany; ^cInstitut für Klinische Chemie, Medizinische Hochschule Hannover, 30625 Hannover, Germany; ^dInstitut für Immunologie, Universitätsklinikum Essen, Universität Duisburg-Essen, 45147 Essen, Germany; ^eInstitut für Virologie, Technische Universität München/Helmholtz Zentrum München, 81675 Munich, Germany; ^fDepartment of Biomedicine, Aarhus University, 8000 Aarhus C, Denmark; ^gDivision of Chronic Inflammation and Cancer, German Cancer Research Center (DKFZ), 69120 Heidelberg, Germany; and ^hGerman Cancer Consortium (DKTK), 69120 Heidelberg, Germany

Edited by Michael Karin, University of California San Diego School of Medicine, La Jolla, CA, and approved August 5, 2019 (received for review December 17, 2018)

The detection of microbes and damaged host cells by the innate immune system is essential for host defense against infection and tissue homeostasis. However, how distinct positive and negative regulatory signals from immune receptors are integrated to tailor specific responses in complex scenarios remains largely undefined. Clec12A is a myeloid cell-expressed inhibitory C-type lectin receptor that can sense cell death under sterile conditions. Clec12A detects uric acid crystals and limits proinflammatory pathways by counteracting the cell-activating spleen tyrosine kinase (Syk). Here, we surprisingly find that Clec12A additionally amplifies type I IFN (IFN-I) responses in vivo and in vitro. Using retinoic acid-inducible gene I (RIG-I) signaling as a model, we demonstrate that monosodium urate (MSU) crystal sensing by Clec12A enhances cytosolic RNA-induced IFN-I production and the subsequent induction of IFN-I-stimulated genes. Mechanistically, Clec12A engages Src kinase to positively regulate the TBK1-IRF3 signaling module. Consistently, Clec12A-deficient mice exhibit reduced IFN-I responses upon lymphocytic choriomeningitis virus (LCMV) infection, which affects the outcomes of these animals in acute and chronic virus infection models. Thus, our results uncover a previously unrecognized connection between an MSU crystal-sensing receptor and the IFN-I response, and they illustrate how the sensing of extracellular damage-associated molecular patterns (DAMPs) can shape the immune response.

Clec12A | type I interferon | C-type lectin receptor | TBK1-IRF3 signaling | LCMV

Innate immune cells express germline-encoded pattern recognition receptors (PRRs) to sense immunological cues from microbes and stressed/dying host cells. Once activated, these PRRs engage intracellular signaling pathways that cooperatively control the production of immune effector molecules, such as inflammatory cytokines and interferons, to tune the host defense mechanisms against the specific invading pathogens, while at same time limiting unwanted immunopathology (1, 2). Signaling PRRs expressed on myeloid cells include the transmembrane Toll-like receptors (TLRs) and C-type lectin receptors, as well as intracellular receptors, such as nucleic acid sensors, Nod-like receptors, and inflammasomes (3). While the individual signaling cascades that are activated by these PRRs have been comprehensively dissected during the last 2 decades (3), the crosstalk between these pathways and the integration of the signals after pathogen detection and upon cell death sensing remain ill-defined.

C-type lectin receptors (CLRs) represent one important PRR family of innate immune cells and recognize both pathogen-associated molecular patterns (PAMPs) and endogenous danger-associated molecular patterns (DAMPs) (4). Based on their intracellular signaling modules, CLRs are broadly grouped into activating and inhibitory receptors (5). Activating CLRs include Dectin-1, Dectin-2, or Mincle, which utilize immunoreceptor

tyrosine-based activation motifs (ITAMs) for intracellular signaling. Following their ligation, membrane-associated Src family kinases (SFKs) (6) are first activated and phosphorylate receptor-associated or coupled ITAM to subsequently recruit and activate the spleen tyrosine kinase (Syk) for innate immune cell activation (7). In contrast, the inhibitory CLRs are characterized by the immunoreceptor tyrosine-based inhibitory motifs (ITIMs). The ligation of inhibitory CLRs also triggers the activation of membrane-associated SFKs that phosphorylate the ITIM tails, which then recruit tyrosine phosphatases, such as SHP-1 and SHP-2, which counteract Syk to negatively modulate cellular activation (8).

Clec12A (also known as MICL, CLL-1, or DCAL-2) is a prototypic ITIM-containing CLR that is predominantly expressed on myeloid cells (9, 10). Earlier studies have demonstrated that Clec12A couples to SHP-1 and SHP-2 after SFK-mediated ITIM phosphorylation (9). Moreover, recent work identified Clec12A as a specific receptor for the detection of cell death under sterile conditions (11). Specifically, uric acid (monosodium urate, MSU) crystals, which are potent DAMPs that alert the immune system to cell death, are Clec12A agonists (11). Consistent with its negative regulatory role in inflammatory pathways, Clec12A can limit

Significance

Viral infections are accompanied by the release of pathogen-associated molecular patterns (PAMPs) during the virus life-cycle and damage-associated molecular patterns (DAMPs) from collateral injured cells. The sensing of viral PAMPs by pattern recognition receptors (PRRs) such as Toll-like receptors RIG-I and cGAS is essential in initiating host antiviral responses, especially the type I interferon (IFN-I) response. Here, we report that the DAMP-sensing C-type lectin receptor Clec12A positively regulates the IFN-I response induced by RIG-I, providing a mechanism of cross-talk between PAMP- and DAMP-triggered signaling pathways. Moreover, this modulatory function of Clec12A has functional consequences in both acute and chronic viral infection in mice.

Author contributions: K.L., K.N., and J.R. designed research; K.L., K.N., V.D., and S.N. performed research and analyzed data; A.L.H. and C.K.H. provided key information for the in vivo experiments; T.W. provided expertise on the RNA-sequencing data analysis; M.H., K.S.L., and J.R. supervised animal experiments; and K.L., K.N., Z.K., and J.R. wrote the paper.

The authors declare no conflict of interest.

This article is a PNAS Direct Submission.

This open access article is distributed under [Creative Commons Attribution-NonCommercial-NoDerivatives License 4.0 \(CC BY-NC-ND\)](https://creativecommons.org/licenses/by-nc-nd/4.0/).

Data deposition: The RNA-seq data have been uploaded to the GEO database (accession no. [GSE134082](https://www.ncbi.nlm.nih.gov/geo/query/acc.cgi?acc=GSE134082)).

¹To whom correspondence may be addressed. Email: j.ruland@tum.de.

This article contains supporting information online at www.pnas.org/lookup/suppl/doi:10.1073/pnas.1821351116/-DCSupplemental.

Published online August 26, 2019.

sterile inflammation by dampening Syk-mediated reactive oxygen species (ROS) production and by preventing the overproduction of proinflammatory cytokines and chemokines, such as tumor necrosis factor (TNF) and CXCL1 (11). In addition, Clec12A has important negative regulatory functions in collagen antibody-induced arthritis, which is another model of sterile inflammation (12). However, the biological functions of Clec12A signaling during infection, which is frequently associated with host cell injury, remain unclear.

The type I IFN (IFN-I) response represents a pivotal defensive mechanism against viral infection. During virus replication, viral nucleic acids are exposed within the host cell and serve as PAMPs that are detected by nucleic acid-sensing PRRs, such as RIG-I, MDA-5, cGAS, TLR3, and TLR7, to induce IFN-I production (13). Subsequently, the binding of IFN-I to the IFN-I receptor (IFNAR) initiates the transcription of IFN-stimulated genes (ISGs) with different effector functions depending on the immunological context (14). Most ISGs exert direct antiviral effects. However, some ISGs, such as programmed death-ligand 1 (PD-L1), counteract the antiviral immune responses during chronic viral infections (15, 16), necessitating the fine-tuning of the IFN-I response. Whereas most viral nucleic acid-sensing pathways induce IFN-I production by engaging the Tank-binding kinase 1 (TBK1)-IFN regulatory factor 3 (IRF3) signaling module (17), it remains unclear how the immunological context in the environment can modulate the IFN-I response.

Here, we surprisingly observed that the uric acid crystal receptor Clec12A functions as a positive modulator of the IFN-I response, which amplifies nucleic acid-sensing PRR signals through the TBK1-IRF3 axis. Furthermore, we report that *Clec12a*^{-/-} mice exhibit increased susceptibility to acute lymphocytic choriomeningitis virus (LCMV) infection and improved virus clearance during chronic LCMV infection in vivo. These results provide insights into the interplay of cell death receptors and IFN-signaling pathways during infection and reveal a previously unrecognized positive regulatory role of an ITIM-containing CLR for IFN-I production.

Results

Clec12A Positively Regulates the Expression of IFN-I-Stimulated Genes. To explore the functions of Clec12A in sterile inflammation, we had induced noninfectious cell death in the mouse thymus via X-ray irradiation in vivo (11). Clec12A ligands will be exposed in such a model either directly by dead thymocytes or due to the resultant inflammation. We observed that the expression of proinflammatory chemokines and cytokines in the thymus was up-regulated in the absence of Clec12A, consistent with the inhibitory role of Clec12A during sterile inflammation (11, 12). In these experiments, we additionally observed substantial decreases in *Ifit3* and *Irf7* expression in the irradiated thymi of *Clec12a*^{-/-} mice (Fig. 1A). Because both *Ifit3* and *Irf7* are strongly induced by IFN-I (14), we became interested in putative functions of Clec12A in regulating the IFN-I response.

As indicated above, IFN-I is strongly induced after cytosolic nucleic acid sensing and is particularly important during viral infection. Therefore, we next investigated potential crosstalks between Clec12A and the RIG-I signaling pathway. To this end, we utilized bone marrow-derived dendritic cells (BMDCs), which express high levels of Clec12A, and stimulated wild-type (WT) cells with either the RIG-I ligand 5'-triphosphate RNA (3pRNA) (18) or the Clec12A agonist MSU crystals. In contrast to RIG-I ligation, cell stimulation with MSU crystals alone was not sufficient to trigger *Ifit3* or *Irf7* expression (Fig. 1B). However, the costimulation of BMDCs with RIG-I ligand and MSU crystals strongly enhanced *Ifit3* and *Irf7* expression in comparison to the sole RIG-I stimulation, and this amplifying response was in large part mediated via Clec12A (Fig. 1C). In addition, the 3pRNA-induced ISG expression was not affected by MSU stimulation in MAVS-deficient BMDCs, indicating that MSU crystal enhances 3pRNA-induced ISG expression via the RIG-I-MAVS pathway (SI Appendix, Fig. S1A).

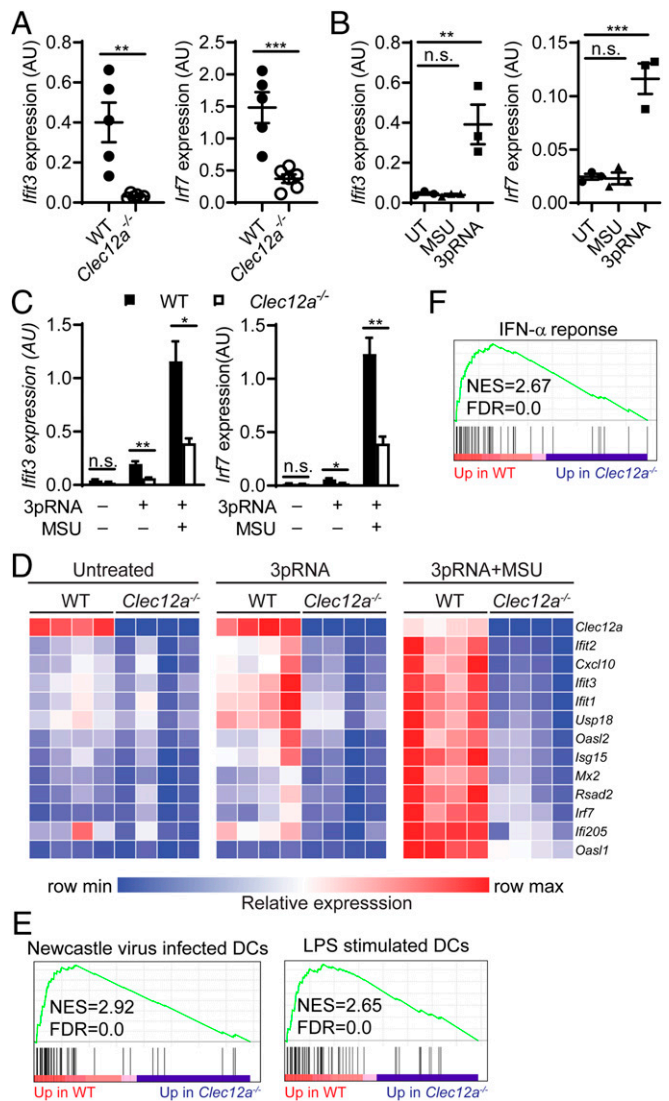


Fig. 1. Clec12A mediates optimal ISG expression. (A) Relative expression of *Ifit3* and *Irf7* in the thymi of whole body-irradiated mice. Data are depicted as the means \pm SEM. Each data point represents 1 biological replicate. Representative data of 2 independent experiments are shown. (B) Relative expression of *Ifit3* and *Irf7* in WT BMDCs left untreated or stimulated with either MSU crystal or 3pRNA for 3 h. Data are depicted as the means of 3 mice per genotype \pm SEM, with each individual data point shown. (C) Relative expression of *Ifit3* and *Irf7* in BMDCs left untreated or stimulated with 3pRNA alone or costimulated with 3pRNA+MSU crystal for 3 h. Data are depicted as the means of 3 mice per genotype \pm SEM. Representative data of 3 independent experiments are shown. (D–F) mRNA isolated from BMDCs treated as in C was subjected to RNA-seq. (D) Heatmap showing the expression profiles of *Clec12a* and putative ISGs that are among the top 100 most down-regulated genes in the costimulated *Clec12a*^{-/-} BMDCs versus WT BMDCs. Data shown are relative FPKM values of individual biological replicates in the RNA-seq. (E and F) Gene set enrichment analysis plots of the differentially expressed genes in the costimulated WT versus *Clec12a*^{-/-} BMDCs. The expression dataset was compared with MSigDB gene set collection C7 (immunological signature, 4,872 gene sets) (E) or collection H (Hallmark gene sets, 50 gene sets) (F). NES, normalized enrichment score; FDR, false discovery rate; AU, arbitrary unit. * $P < 0.05$, *** $P < 0.01$, **** $P < 0.001$, n.s., not significant, 2-tailed t test (A and C), and 1-way ANOVA with post hoc Tukey's test (B).

Next, we globally explored the modulatory roles of Clec12A signaling in 3pRNA-induced ISG expression by performing RNA-sequencing (RNA-seq) and compared the gene expression signatures of untreated, 3pRNA-stimulated, and 3pRNA and MSU

crystal-costimulated WT and *Clec12a*^{-/-} BMDCs. Bioinformatic analysis of the transcriptome data using Cufflinks (19) demonstrated that more than 600 genes were significantly down-regulated in the 3pRNA plus MSU crystal-costimulated *Clec12a*^{-/-} BMDCs in comparison to the 3pRNA plus MSU crystal-costimulated WT cells. In addition to *Ifit3* and *Irf7*, these down-regulated genes included multiple other ISGs, such as *Ifit2*, *Usp18*, *Isg15*, and *Rsad2* (Fig. 1D) (14). Additional qPCR analysis further revealed that the 3pRNA-induced expression of *Ifit1* was also down-regulated in MSU crystal-costimulated *Clec12a*^{-/-} BMDCs compared to WT cells (SI Appendix, Fig. S1B), although expression of IFN-I genes was not identified in our primary RNA-seq data due to low read coverage. Subsequently, we performed gene set enrichment analysis (GSEA) against the MSigDB gene set collection C7 (immunological signatures) to identify biological processes that are regulated by Clec12A signaling under our experimental conditions (20). Notably, the gene sets significantly enriched in the 3pRNA-stimulated WT BMDCs in comparison to *Clec12a*^{-/-} cells consisted of genes that can be induced by Newcastle disease virus (NDV) infection and lipopolysaccharide (LPS) stimulation (Fig. 1E). Importantly, the most significant enrichment of these gene sets occurred under the situation of 3pRNA plus MSU crystal costimulation (SI Appendix, Fig. S1C). As both the “NDV infection” and “LPS stimulation” gene sets include a strong IFN-I gene expression signature, these data further support a positive regulatory role for Clec12A signaling in the amplification of the IFN-I response in our experimental settings. In line with these observations, the hallmark gene set with the signature “IFN- α response” was also significantly enriched in the 3pRNA and MSU crystal-costimulated WT BMDCs compared with that of costimulated *Clec12a*^{-/-} cells when we applied GSEA against the MSigDB Collection H (Hallmark pathways) (Fig. 1F). Thus, these genetic experiments in primary cells demonstrate that Clec12A possesses a previously unrecognized function that is required for optimal ISG induction after thymus irradiation as well as for the amplification of the IFN-I response in innate immune cells after RIG-I activation.

Clec12A Regulates IFN-I Production but Not IFN-I Receptor Signaling.

Key for the expression of ISGs is the activation of the transcription factor STAT1. Upon stimulation of the IFN-I receptor with IFN-I, STAT1 is phosphorylated at position Y701, resulting in a heterodimerization of STAT1 with STAT2 and the formation of the transcriptionally active ISGF3, which directs the expression of ISGs (14). To gain insights into the molecular mechanisms by which Clec12A regulates ISG expression, we first studied STAT1 phosphorylation upon 3pRNA treatment, with or without MSU crystal costimulation. Consistent with the decreased expression of ISGs, the *Clec12a*^{-/-} cells also exhibited reduction of STAT1 Y701 phosphorylation upon 3pRNA transfection (Fig. 2A). This effect was observed with and without MSU crystal costimulation (Fig. 2A).

The reduced STAT1 phosphorylation of Clec12A-deficient cells could be either a direct consequence of impaired intracellular IFN-I receptor signaling or a secondary effect of reduced IFN-I production leading to decreased autocrine IFN-I receptor stimulation or paracrine stimulation of neighboring cells. To explore these possibilities, we next stimulated WT and *Clec12a*^{-/-} BMDCs with increasing concentrations of recombinant IFN- β , with or without MSU crystal costimulation. Subsequent Western blot analysis revealed regular STAT1 phosphorylation in *Clec12a*^{-/-} BMDCs under all tested conditions (Fig. 2B). These results were further corroborated by the observation that the *Ifit3* and *Irf7* transcripts were also regularly induced in *Clec12a*^{-/-} BMDCs upon recombinant IFN- β treatment (Fig. 2C). Thus, the deficiency of Clec12A does not directly influence the IFN-I receptor pathway. In contrast, the production of IFN-I upon RIG-I stimulation, with or without MSU crystal costimulation, was significantly impaired in the absence of Clec12A (Fig. 2D), demonstrating that Clec12A is required for optimal IFN-I production upon RIG-I stimulation.

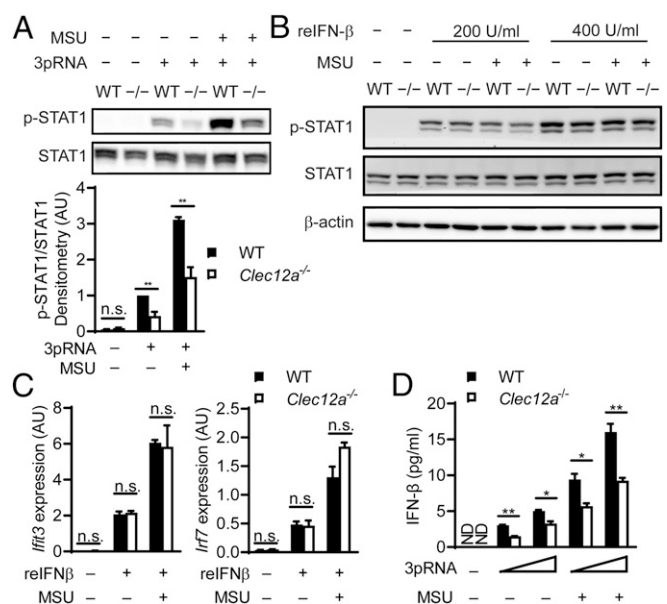


Fig. 2. Clec12A regulates IFN-I production but does not affect IFN-I receptor signaling. (A) Immunoblot analysis of STAT1 Y701 phosphorylation in BMDCs left untreated or stimulated with 3pRNA alone or costimulated with 3pRNA+MSU crystal for 2 h. Total STAT1 served as the control. Also shown is the densitometric quantification of phosphorylated STAT1 relative to the total STAT1 level from 3 experiments. Data were normalized to WT BMDCs stimulated with 3pRNA alone. (B) Immunoblot analysis of STAT1 Y701 phosphorylation in BMDCs left untreated or stimulated with the indicated dose of recombinant IFN- β for 30 min, with or without MSU crystal costimulation. Total STAT1 and β -actin served as controls. Representative data of 3 independent experiments are shown. (C) Relative expression of *Ifit3* and *Irf7* in BMDCs left untreated or stimulated with recombinant IFN- β (200 U/ml) for 3 h, with or without MSU crystal costimulation. Data are depicted as the means of 5 mice per genotype + SEM. Representative data of 3 independent experiments are shown. (D) IFN- β levels in the cell-free supernatant of BMDCs left untreated or stimulated with 3pRNA (0.2 μ g/mL and 0.5 μ g/mL) alone or costimulated with 3pRNA+MSU crystal for 6 h. Data are depicted as the means of 3 mice per genotype + SEM. Representative data of 2 independent experiments are shown. reIFN- β , recombinant IFN- β ; ND, not detected; AU, arbitrary unit. * P < 0.05, ** P < 0.01, n.s., not significant, 2-tailed t test (A, C, and D).

Clec12A Amplifies the TBK1-IRF3 Axis of RIG-I-Induced IFN-I Production through Activating SFKs.

The expression of IFN-I in response to RIG-I ligation is controlled by the transcription factor IRF3, which is activated by the serine kinase TBK1 (21). This TBK1-IRF3 signaling module serves as a point of convergence for several IFN-I-driving innate signaling pathways (17). To test if Clec12A signaling could modulate the TBK1-IRF3 signaling axis, we next costimulated WT and *Clec12a*^{-/-} BMDCs with 3pRNA and MSU crystals. As expected, this treatment triggered the phosphorylation of TBK1 at S172, which is indicative of TBK1 activation (Fig. 3A). Full TBK1 activation was dependent on Clec12A (Fig. 3A). In line with these results, the costimulation-induced phosphorylation of IRF3 at S396 was also impaired in *Clec12a*^{-/-} cells (Fig. 3B). As the levels of lactate dehydrogenase (LDH) in the supernatants of the stimulated cells did not differ between WT and *Clec12a*^{-/-} BMDCs (SI Appendix, Fig. S2), the differences in TBK1/IRF3 signaling were not due to a potential increase in the death of stimulated *Clec12a*^{-/-} cells. Because the phosphorylation of IRF3 by TBK1 induces its transcriptional activity (22), these findings elucidate the impaired IFN-I production of 3pRNA+MSU crystal-stimulated *Clec12a*^{-/-} deficient cells.

Src family tyrosine kinases (SFKs) can directly phosphorylate TBK1 at Y179, which facilitates the autophosphorylation of TBK1 at S172 and increases the TBK1 kinase activity (23). Given that SFKs can be activated by CLR (6), we next tested whether

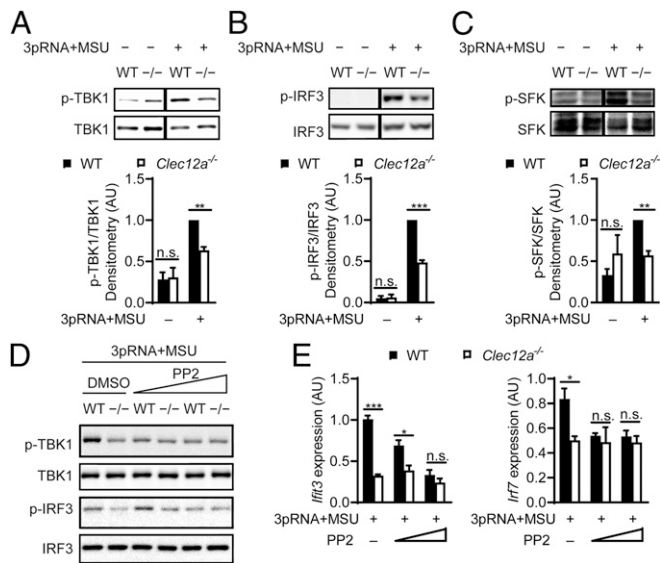


Fig. 3. Clec12A positively regulates the RIG-I-activated TBK1-IRF3 signaling axis through modulating SFK. (A–C) Immunoblot analysis of TBK1 S172 phosphorylation (A) and IRF3 S396 phosphorylation (B) or SFK Y416 phosphorylation (C) in BMDCs left untreated or costimulated with 3pRNA+MSU crystal for 2 h. Total TBK1, IRF3, and Src were used as controls for respective phosphorylated proteins. Also shown is the densitometric quantification of phosphorylated proteins relative to the respective controls from 3 experiments. Data were normalized to WT BMDCs costimulated with 3pRNA and MSU crystal. (D and E) BMDCs pretreated with PP2 (5 and 10 μ M) and subsequently costimulated with 3pRNA+MSU crystal for 2 (D) or 3 (E) h were subjected to immunoblot analysis of TBK1 S172 and IRF3 S396 phosphorylation, with total TBK1 and IRF3 used as controls, respectively (D), or relative gene expression analysis of *Ifit3* and *Irf7*. The means of 3 or 4 mice per genotype + SEM are depicted (E). Data shown are representative of 3 experiments (D). * $P < 0.05$, ** $P < 0.01$, *** $P < 0.001$, n.s., not significant, 2-tailed *t* test (A–C and E).

Clec12A could modulate TBK1 activity via SFK signaling. Therefore, we again costimulated WT and *Clec12a*^{−/−} BMDCs with MSU crystals plus 3pRNA and investigated Y416 phosphorylation within the Src kinase domain (and the corresponding analogous sites within other SFKs) by Western blot analysis as a measurement for SFK activation (24). Indeed, 3pRNA and MSU crystal costimulation triggered SFK activation in BMDCs in a Clec12A-dependent manner (Fig. 3C). To test whether the Clec12A-mediated SFK activation would negatively modulate the IFN-I response, we pretreated WT and Clec12A-deficient BMDCs with the SFK inhibitor PP2 (25) prior to 3pRNA and MSU crystal costimulation. Inhibition of SFK abolished the Clec12A-dependent increases in TBK1 and IRF3 phosphorylation in the WT BMDCs (Fig. 3D). Moreover, the pharmacological blocking of SFK activity (25) also inhibited the Clec12A-dependent enhancement of ISG expression, with or without MSU costimulation (Fig. 3E and *SI Appendix, Fig. S3A*), indicating that the amplification of the RIG-I-triggered IFN-I production via Clec12A is mediated at least in part via the activation of SFKs. Since Clec12A can recruit phosphatases such as SHP-1/2 via its ITIM motif, we also pretreated the BMDCs with the SHP-1/2 inhibitor NSC-87877 before cell stimulation with 3pRNA+MSU. However, SHP-1/2 inhibition did not restore the defective expression of *Ifit3* in the Clec12A-deficient BMDCs and did not diminish *Ifit3* expression in the WT cells (*SI Appendix, Fig. S3B*), indicating that the Clec12A-associated phosphatases are dispensable for these processes, which is consistent with the activation of SFK being upstream of SHP-1/2 recruitment.

Clec12A Regulates IFN-I Responses during Virus Infection In Vivo. Because IFN-I production and ISG expression are particularly important for host immunity against viral infection, we next

investigated the function of Clec12A in acute or chronic viral infection. To this end, we used the RNA virus LCMV, which triggers RIG-I-dependent IFN-I production, as a model (26). We infected WT and Clec12A-deficient mice with 2 LCMV strains: the LCMV-WE strain, which causes acute infection that can be cleared by immune-competent mice within 1 or 2 wk, and the LCMV-Docile strain, which establishes a chronic infection in adult mice that can persist for months (27).

The infection of WT mice with 200 plaque-forming units (PFU) of LCMV-WE triggers a profound production of IFN- α measured in the serum (Fig. 4A). However, in the absence of Clec12A, this IFN-I response was significantly reduced (Fig. 4A), highlighting a positive regulatory role for Clec12A in IFN-I response upon viral infection in vivo. Moreover, and consistent with the critical function of IFN-I for antiviral host protection, the *Clec12a*^{−/−} mice exhibited significantly higher viral loads on day 14 postinfection of 2×10^6 PFU of LCMV-WE, as determined by measuring the viral NP gene copy number in the liver homogenates (Fig. 4B). This elevated viral titer in *Clec12a*^{−/−} mice was also consistently associated with an increase in LCMV-WE-triggered liver damage (Fig. 4C) (28), which was monitored over time by examining the activity of the liver enzymes AST and ALT released from dying hepatocytes.

Next, we i.v. injected 2×10^4 PFU of LCMV-Docile to study the role of Clec12A under conditions of chronic viral infection. Two days after infection, we again detected significantly decreased levels of IFN- α in the sera of *Clec12a*^{−/−} mice (Fig. 4D). Noteworthy, during chronic LCMV infection, prolonged IFN-I signaling induces immunosuppressive programs that promote virus persistence, and an attenuated IFN-I response at early phases can facilitate later viral clearance by the host (15, 16). In line with the reduced IFN-I production during the early phase of

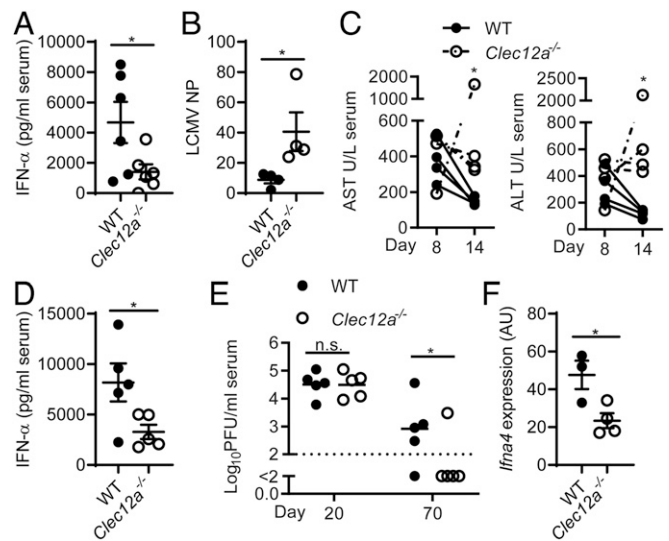


Fig. 4. Function of Clec12A during LCMV infection in vivo. (A) Serum level of IFN- α 2 d after infection of 200 PFU of LCMV-WE. (B) Relative number of LCMV-NP genes in the liver homogenates of mice 14 d after infection of 2×10^6 PFU of LCMV-WE. Data are relative to those of liver β -actin. (C) Serum levels of liver enzyme AST and ALT 8 and 14 d after infection of 2×10^6 PFU of LCMV-WE. The results from the same mouse are connected by a line. (D and E) WT and *Clec12a*^{−/−} mice were i.v. infected with 2×10^4 PFU of LCMV-Docile. (D) Serum level of IFN- α 2 d after infection. (E) Virus titer in the serum at indicated time points after infection. The dashed line indicates the detection limit of the plaque assay. (F) Relative expression of *Ifna4* in lung tissues of mice 4 d postinfection with 6×10^5 PFU of influenza PR8. Data are relative to those of *Gapdh*. Each symbol represents an individual mouse; small horizontal lines indicate the means, and error bars indicate the SEM (A–F). Data of 1 experiment in each case are presented. * $P < 0.05$, 2-tailed *t* test (A, B, D, and F), 1-tailed *t* test (E) and 2-tailed Mann–Whitney test (C).

LCMV-Docile infection, the *Clec12a*^{-/-} mice exhibited more efficient virus clearance by day 70 postinfection in comparison to the WT controls (Fig. 4E). Thus, together, these infection experiments demonstrate that Clec12A signaling controls the level of the IFN-I response and its respective biological consequences during acute or chronic viral infections in vivo.

To probe the role of Clec12A in modulating IFN-I response beyond LCMV infection in vivo, we additionally infected *Clec12a*^{-/-} mice with influenza virus, which is another RNA virus that elicits a local IFN-I response via the RIG-I pathway (29). The predominant IRF3-responsive IFN- α subtype in the mouse is the *Ifna4* (30). Indeed, upon influenza virus infection, *Ifna4* expression was significantly reduced in the lung tissues of *Clec12a*^{-/-} mice as compared to their WT counterparts (Fig. 4F), further demonstrating that Clec12A is required for optimal IFN-I responses upon virus infections in vivo.

Discussion

In this study, we demonstrate an unexpected positive regulatory function of the ITIM receptor Clec12A on the production of IFN-I and the subsequent regulation of the IFN-I response gene expression signature. This Clec12A-mediated pathway can amplify signals elicited by the RNA sensor RIG-I through the MAVS pathway upon MSU crystal detection in vitro and controls the respective host responses to acute and chronic viral infection in vivo.

Critical for IFN production in response to viral infection or sensing of foreign cytosolic nucleic acids is the activation of the kinase TBK1 and the subsequent engagement of the transcription factor IRF3. A recent report has demonstrated that the activation of SFKs can potentiate TBK1 kinase activity after viral infection (23). In line with these findings, our data indicate that the mechanism by which Clec12A amplifies the IFN responses is triggered via SFK activity, as the Clec12A-mediated enhancement of TBK1 activation and downstream IRF3 phosphorylation after MSU crystal detection are abolished by pan-SFK inhibitor PP2 treatment. SFK activation by CLR is in general a first step in the signaling cascades for the engagement of downstream pathways. It is necessary for the subsequent ITIM or ITAM phosphorylation for the recruitment of SHP-1/SHP-2 (inhibitory ITIM receptors) or Syk (activating ITAM receptors). Because pharmacological SHP-1/2 inhibition does not affect Clec12A-regulated ISG expression, we hypothesize that Clec12A signaling bifurcates at the level of SFK activation, such that one branch activates TBK1 to potentiate IFN-I response, whereas the other phosphorylates the ITIM to mediate SHP-1/2 recruitment and counter regulation of Syk as we have reported previously (11). Although the precise mechanisms of SFK activation by Clec12A are unresolved, the detection of uric acid in its crystalline form likely leads to Clec12A clustering and membrane reshuffling with subsequent SFK activation, similar to the activation of SFKs by the prototypic CLR Dectin-1 (31). In this study, we have focused our efforts on the interaction between Clec12A and RIG-I signaling. However, because other nucleic acid-sensing innate immune pathways, such as the cGAS-STING and TLR3/4-TRIF cascades, also activate the IFN-I-response via the TBK1-IRF3 module, it is possible that these pathways could also be modulated by Clec12A, which needs to be investigated in future studies. The fact that Clec12A does not modulate only RNA virus-sensing pathways is already indicated by our initial observation that Clec12A amplifies the IFN-I response during sterile inflammation in irradiated thymus.

In vivo, we found impaired virus-induced IFN-I production and ISG expression in the absence of Clec12A with respective functional consequences. During acute LCMV infection, Clec12A-deficient mice exhibited not only reduced IFN-I levels but also increased LCMV titers, consistent with the fact that many ISGs block key steps in the virus replication cycle, including the transition of virus from the late endosome or lysosome to the cytosol, or the budding of enveloped viruses (14). However, during chronic LCMV infection, prolonged IFN-I signaling can facilitate

virus persistence by inducing the expression of negative immune regulators, such as programmed death-ligand 1 and IL-10 (15, 16). In line with these facts, we also observed effects on LCMV clearance during chronic infection caused by the Clec12A deficiency. Furthermore, in first experiments with influenza virus, we additionally demonstrated that Clec12A regulates IFN-I responses during infection with this virus indicating that the function of Clec12A in IFN-I regulation is not restricted to a single virus family.

As Clec12A is a known sensor of damaged cells (11), it is conceivable that in the context of viral infection, Clec12A can be activated by dead host cells or associated DAMPs, such as uric acid crystals. During the initial phase of a viral infection, proinflammatory cytokine and IFN-I responses can be simultaneously induced to shape and amplify the antiviral immune response. However, if these early measures of the innate immune system are not sufficient to clear the virus, the subsequent cell damage will create an environment that can additionally activate Clec12A. Previously, Clec12A has been shown to limit proinflammatory responses, including immune cell migration and proinflammatory cytokine/chemokine production to limit immunopathology (11). Now, we additionally report that Clec12A positively regulates the IFN-I response. Collectively, we speculate that Clec12A could serve as a molecular scout during viral infection that instructs the immune system to curb inflammatory immunopathology and at the same time amplifies the IFN-I response and ISG expression, which are tailored to block virus replication (14).

Interestingly, cells from different host tissues vary in their capacity to crosslink and activate Clec12A (10). Moreover, while Clec12A clearly recognizes uric acid crystals, it can presumably sense additional unknown endogenous ligands from damaged cells (11). Therefore, in a given infectious context, the amount of Clec12A activation might depend on the specific tissue environment and the local availability of Clec12A ligands. We used MSU crystal as one bona fide Clec12A agonist (11) in our experiments. However, MSU crystals can also activate the NLRP3 inflammasome and the kinase Syk via membrane cholesterol interactions (32, 33) to modulate innate immunity. Although we provide clear data that Clec12A controls the IFN-I response both in vitro and in vivo, Clec12A-independent MSU effects could even further modulate the IFN-I response. Moreover, it is in principle conceivable that Clec12A could sense certain viral structures or modulate the innate immune response via ligand-independent tonic signals, but further studies are required to explore these possibilities.

Initially, we were surprised to observe that an inhibitory ITIM-containing immune receptor would amplify ISG expression. Yet, recent work independently reported that DCIR (also known as Clec4A2), another ITIM-containing CLR that closely clusters with Clec12A in the human and murine genomes (8), could positively regulate the IFN-I response during *Mycobacteria tuberculosis* infection (34). As with Clec12A, DCIR is expressed on BMDCs (35) and can also dampen sterile inflammation in the collagen antibody-induced arthritis model (36). DCIR can recognize a variety of fucose/mannose-containing carbohydrate moieties of both endogenous and exogenous origins, including the gp140 glycoprotein of HIV (37). Although DCIR is similarly required for the optimal transcription of IFN-I signature genes, unlike Clec12A, it does not directly regulate IFN-I production, but rather modulates the IFN-I response by sustaining IFN-I signaling after IFN-I receptor ligation. The distinct yet converging molecular mechanisms of IFN-I response regulation by Clec12A and DCIR indicate that several ITIM-containing CLRs have evolved to modulate the IFN-I response during infection.

In conclusion, within this study, we have established a positive regulatory function of Clec12A in the IFN-I response on a clean genetic basis and a principle mechanism by which endogenous danger signals detected by the innate immune system can be translated into fine-tuned immune responses to infection. Because the genetic loss of Clec12A can enhance protective immunity in a model of chronic LCMV infection, it would be of interest to explore whether Clec12A inhibition could also be beneficial during clinically relevant persistent infections with viruses such as HIV or

HCV, which also exhibit signs of chronic IFN-I signaling (38, 39). Moreover, because a robust induction of IFN-I responses is critical to trigger radiation-induced antitumor immunity (40), and considering that Clec12A potentiates ISG expression during radiation-induced sterile inflammation, future studies that explore the role of Clec12A in cancer radiotherapy are warranted.

Materials and Methods

Additional methods are presented in *SI Appendix, Extended Materials and Methods*.

Mice. *Clec12a*^{-/-} mice were described previously (11). For in vivo experiments, age- and sex-matched WT and *Clec12a*^{-/-} mice were cohoused for at least 1 mo prior to the experiments. All animal work was conducted in accordance with the German federal animal protection laws and was approved by the Institutional Animal Care and Use Committee at the Technical University of Munich or was authorized by Veterinäramt Nordrhein-Westfalen (Düsseldorf, Germany).

Cell Culture and Stimulation. BMDCs were differentiated from bone marrow aspirates as previously described (41). Cells were kept in RPMI 1640 with 5% FCS during stimulation. Lipofectamine 2000 (Invitrogen) was used to transfect 3pRNA into BMDCs.

1. J. S. Bezradica, R. K. Rosenstein, R. A. DeMarco, I. Brodsky, R. Medzhitov, A role for the ITAM signaling module in specifying cytokine-receptor functions. *Nat. Immunol.* **15**, 333–342 (2014).
2. X. Cao, Self-regulation and cross-regulation of pattern-recognition receptor signalling in health and disease. *Nat. Rev. Immunol.* **16**, 35–50 (2016).
3. S. W. Brubaker, K. S. Bonham, I. Zanoni, J. C. Kagan, Innate immune pattern recognition: A cell biological perspective. *Annu. Rev. Immunol.* **33**, 257–290 (2015).
4. D. Sancho, C. Reis e Sousa, Signaling by myeloid C-type lectin receptors in immunity and homeostasis. *Annu. Rev. Immunol.* **30**, 491–529 (2012).
5. I. M. Dambaza, G. D. Brown, C-type lectins in immunity: Recent developments. *Curr. Opin. Immunol.* **32**, 21–27 (2015).
6. C. A. Lowell, Src-family and Syk kinases in activating and inhibitory pathways in innate immune cells: Signaling cross talk. *Cold Spring Harb. Perspect. Biol.* **3**, a002352 (2011).
7. A. Mócsai, J. Ruland, V. L. J. Tybulewicz, The SYK tyrosine kinase: A crucial player in diverse biological functions. *Nat. Rev. Immunol.* **10**, 387–402 (2010).
8. P. Redelinghuys, G. D. Brown, Inhibitory C-type lectin receptors in myeloid cells. *Immunol. Lett.* **136**, 1–12 (2011).
9. A. S. J. Marshall *et al.*, Identification and characterization of a novel human myeloid inhibitory C-type lectin-like receptor (MICL) that is predominantly expressed on granulocytes and monocytes. *J. Biol. Chem.* **279**, 14792–14802 (2004).
10. E. Pyž *et al.*, Characterisation of murine MICL (CLEC12A) and evidence for an endogenous ligand. *Eur. J. Immunol.* **38**, 1157–1163 (2008).
11. K. Neumann *et al.*, Clec12a is an inhibitory receptor for uric acid crystals that regulates inflammation in response to cell death. *Immunity* **40**, 389–399 (2014).
12. P. Redelinghuys *et al.*, MICL controls inflammation in rheumatoid arthritis. *Ann. Rheum. Dis.* **75**, 1386–1391 (2016).
13. D. Goubau, S. Deddouche, C. Reis e Sousa, Cytosolic sensing of viruses. *Immunity* **38**, 855–869 (2013).
14. W. M. Schneider, M. D. Chevillotte, C. M. Rice, Interferon-stimulated genes: A complex web of host defenses. *Annu. Rev. Immunol.* **32**, 513–545 (2014).
15. E. B. Wilson *et al.*, Blockade of chronic type I interferon signaling to control persistent LCMV infection. *Science* **340**, 202–207 (2013).
16. J. R. Teijaro *et al.*, Persistent LCMV infection is controlled by blockade of type I interferon signaling. *Science* **340**, 207–211 (2013).
17. S. Liu *et al.*, Phosphorylation of innate immune adaptor proteins MAVS, STING, and TRIF induces IRF3 activation. *Science* **347**, aaa2630 (2015).
18. A. Pichlmair *et al.*, RIG-I-mediated antiviral responses to single-stranded RNA bearing 5'-phosphates. *Science* **314**, 997–1001 (2006).
19. C. Trapnell *et al.*, Differential gene and transcript expression analysis of RNA-seq experiments with TopHat and Cufflinks. *Nat. Protoc.* **7**, 562–578 (2012).
20. A. Subramanian *et al.*, Gene set enrichment analysis: A knowledge-based approach for interpreting genome-wide expression profiles. *Proc. Natl. Acad. Sci. U.S.A.* **102**, 15545–15550 (2005).
21. K. A. Fitzgerald *et al.*, IKKepsilon and TBK1 are essential components of the IRF3 signaling pathway. *Nat. Immunol.* **4**, 491–496 (2003).
22. M. J. Servant *et al.*, Identification of the minimal phosphoacceptor site required for in vivo activation of interferon regulatory factor 3 in response to virus and double-stranded RNA. *J. Biol. Chem.* **278**, 9441–9447 (2003).

Immunoblot Analysis. BMDC cells stimulated for indicated times were lysed in Laemmli buffer or Nonidet P-40 buffer (for SFK detection) and subjected to standard immunoblot analysis. Quantification of protein bands was performed by densitometry using ImageJ software. Densitometry data of target proteins were first compared to those of the respective loading controls and were subsequently normalized to specific treatment conditions, as indicated.

Statistical Analysis. Data were analyzed and plotted by using GraphPad Prism (GraphPad software, La Jolla, California). When the data were normally distributed, unpaired *t* tests (2-tailed) were used to compare 2 means. When the data did not follow a normal distribution, Mann-Whitney tests were used to compare 2 means. Analysis across more than 2 groups within a single dataset was performed using 1-way ANOVA with post hoc Tukey's test.

ACKNOWLEDGMENTS. We thank Hendrik Poeck for sharing MAVS-deficient bone marrow cells; Nicole Prause, Tanja Neumayer, and Kerstin Burmeister for providing excellent technical assistance; Silvia Thöne for critical manuscript editing; and David M. Underhill for providing laboratory resources and valuable scientific discussion during paper revision. This work was supported by research grants from the Deutsche Forschungsgemeinschaft (DFG) (SFB 1054/B01, Projektnummer 360372040 – SFB 1335, Projektnummer 395357507 – SFB 1371, TRR 237/A10, and RU 695/9–1) and the European Research Council (ERC) (FP7, Grant Agreement 322865) (to J.R.). We thank the high-throughput-sequencing unit of the Genomics and Proteomics Core Facility, German Cancer Research Center (DKFZ), for providing excellent sequencing services.

23. X. Li *et al.*, The tyrosine kinase Src promotes phosphorylation of the kinase TBK1 to facilitate type I interferon production after viral infection. *Sci. Signal* **10**, eaee0435 (2017).
24. W. Xu, A. Doshi, M. Lei, M. J. Eck, S. C. Harrison, Crystal structures of c-Src reveal features of its autoinhibitory mechanism. *Mol. Cell* **3**, 629–638 (1999).
25. J. H. Hanke *et al.*, Discovery of a novel, potent, and Src family-selective tyrosine kinase inhibitor. Study of Lck- and FynT-dependent T cell activation. *J. Biol. Chem.* **271**, 695–701 (1996).
26. S. Zhou *et al.*, Induction and inhibition of type I interferon responses by distinct components of lymphocytic choriomeningitis virus. *J. Virol.* **84**, 9452–9462 (2010).
27. V. Duhau *et al.*, Virus-specific antibodies allow viral replication in the marginal zone, thereby promoting CD8(+) T-cell priming and viral control. *Sci. Rep.* **6**, 19191 (2016).
28. R. M. Zinkernagel *et al.*, T cell-mediated hepatitis in mice infected with lymphocytic choriomeningitis virus. Liver cell destruction by H-2 class I-restricted virus-specific cytotoxic T cells as a physiological correlate of the 51Cr-release assay? *J. Exp. Med.* **164**, 1075–1092 (1986).
29. H. Kato *et al.*, Differential roles of MDA5 and RIG-I helicases in the recognition of RNA viruses. *Nature* **441**, 101–105 (2006).
30. I. Marié, J. E. Durbin, D. E. Levy, Differential viral induction of distinct interferon- α genes by positive feedback through interferon regulatory factor-7. *EMBO J.* **17**, 6660–6669 (1998).
31. H. S. Goodridge *et al.*, Activation of the innate immune receptor Dectin-1 upon formation of a 'phagocytic synapse'. *Nature* **472**, 471–475 (2011).
32. F. Martinon, V. Pettrilli, A. Mayor, A. Tardivel, J. Tschopp, Gout-associated uric acid crystals activate the NALP3 inflammasome. *Nature* **440**, 237–241 (2006).
33. G. Ng *et al.*, Receptor-independent, direct membrane binding leads to cell-surface lipid sorting and Syk kinase activation in dendritic cells. *Immunity* **29**, 807–818 (2008).
34. A. Troegeler *et al.*, C-type lectin receptor DCIR modulates immunity to tuberculosis by sustaining type I interferon signaling in dendritic cells. *Proc. Natl. Acad. Sci. U.S.A.* **114**, E540–E549 (2017).
35. E. E. Bates *et al.*, APCs express DCIR, a novel C-type lectin surface receptor containing an immunoreceptor tyrosine-based inhibitory motif. *J. Immunol.* **163**, 1973–1983 (1999).
36. N. Fujikado *et al.*, Dcir deficiency causes development of autoimmune diseases in mice due to excess expansion of dendritic cells. *Nat. Med.* **14**, 176–180 (2008).
37. K. Bloem *et al.*, DCIR interacts with ligands from both endogenous and pathogenic origin. *Immunol. Lett.* **158**, 33–41 (2014).
38. C. R. Bolen *et al.*, The blood transcriptional signature of chronic hepatitis C virus is consistent with an ongoing interferon-mediated antiviral response. *J. Interferon Cytokine Res.* **33**, 15–23 (2013).
39. B. Jacquelin *et al.*, Nonpathogenic SIV infection of African green monkeys induces a strong but rapidly controlled type I IFN response. *J. Clin. Invest.* **119**, 3544–3555 (2009).
40. L. Deng *et al.*, STING-dependent cytosolic DNA sensing promotes radiation-induced type I interferon-dependent antitumor immunity in immunogenic tumors. *Immunity* **41**, 843–852 (2014).
41. S. Roth *et al.*, Vav proteins are key regulators of card9 signaling for innate antifungal immunity. *Cell Rep.* **17**, 2572–2583 (2016).